Experimental Investigation of a Novel Dissolution Model

Medhat A. Toukhy, Steven G. Hansen, Rodney J. Hurditch
OCG Microelectronic Materials, Inc., 200 Massasoit Ave., E. Providence, RI 02914

Chris A. Mack
FINLE Technologies, P.O. Box 261034, Plano, TX 75026

Abstract

Mack recently proposed a new kinetically-based 5-parameter model for positive photoresist bulk dissolution. The present work tests its physical assumptions by comparing its predictions with DRM measurements of seven different PAC/novolak formulations, each at several different PAC loadings. Although substantial qualitative agreement between the predictions and experiments is seen, quantitative agreement is poor. The most likely explanations for the quantitative difficulties are: 1) the assumptions that inhibition by the PAC and enhancement by the photo-acid can be treated independently and multiplicatively, apparently fail, 2) side reactions and intermediates are neglected by the model, and 3) complex PAC isomeric distributions and associated complex inhibition/enhancement effects are also neglected. The dissolution rate equation derived by the model does exhibit excellent flexibility in fitting actual bulk dissolution rate curves. This reason alone is sufficient to recommend its inclusion in commonly-used simulation programs such as PROLITH/2 and SAMPLE. The present work shows that significant errors can result in simulations by using simple dissolution rate equation which are unable to accurately describe observed bulk dissolution data.

1. Introduction

Computer simulation of photolithography is becoming a more reliable tool. It can assist lithographic engineers in efficiently optimizing their resist processes by evaluating the performance of different resist products under a variety of process conditions. Equipment and mask designers can also benefit from simulation by testing advanced or hypothetical configurations.

The reliability of simulation results is greatest when an accurate description of the resist dissolution rate characteristics is used. This information is collected experimentally by a development rate monitor (DRM). Commonly used 3 and 4 parameter equations are often inadequate, only crudely fitting the DRM data, and thus important details of the dissolution can be lost and artifacts introduced. This problem is easily addressed by choosing rate equations with more adjustable parameters[1], however, all physical intuition is then lost. Therefore, physically-based dissolution models which adequately fit the experimental dissolution data are needed. A successful model of this type would not only improve simulation accuracy but would also bridge the gap between resist chemistry, formulation and lithographic performance. Such a dissolution model was recently proposed by Mack[2], and is experimentally tested in this paper. This model, takes the following form:

$$R(M)=R_{resin}\{1+k_{enh}(1-M)^{n}\}/\{1+k_{inh}(M)^{l}\} \quad (1)$$

Where, R(M) is the resist dissolution rate for the normalized PAC concentration (M), R_{resin} is the development rate of the resin alone, k_{enh} and k_{inh} are effective rate constants for the enhancement constant and inhibition mechanisms and n and l are the effective reaction orders for enhancement and inhibition, respectively. This equation defines maximum and minimum dissolution rates:

$$\text{Unexposed PAC} \quad ; M=1 , \quad R_{min}=R_{resin}/(1+k_{inh}) \quad (2)$$

$$\text{fully bleached PAC} \quad ; M=0 , \quad R_{max}=R_{resin}(1+k_{enh}) \quad (3)$$

 0-8194-0827-1/92/$4.00

The development rate expression is therefore characterized by five parameters: R_{resin}, n, l, and either R_{min} and R_{max} or k_{inh} and k_{enh}.

2. Experimental

2.1 Strategy of testing the dissolution model

The strategy followed to test the model was to examine its applicability to several experimental resist formulations designed to provide a wide range of inhibition/discrimination behaviors. The dissolution and inhibition mechanisms of a given resist system are assumed to be independent of PAC concentration, at least within the range of the formulated resists. Therefore, one would expect that a single set of dissolution inhibition and enhancement reaction orders and rate constants would apply for each specific resist system. Each resist system is based on one novolak resin formulated with different loadings of the same PAC. Seven different novolak/PAC combinations totaling 23 resist formulations were prepared and their dissolution curves measured via DRM.

2.2 Selection of novolak, PACs and formulations

Three novolaks differing in their dissolution rates and compositions were chosen for this test. The novolaks were also chosen to provide different interactions with the PAC. Two cresol/formaldehyde novolaks were prepared: the starting materials were 60% m-cresol/40% p-cresol (F), and 40% m-cresol/60% p-cresol (N), respectively. Also a xylenol type novolak (X) was used. Due to the higher reactivity of m-cresol than p-cresol with formaldehyde, the final cresol compositions of these novolaks were: 80% m-cresol/20% p-cresol for novolak (F), and 50% m-cresol/50% p-cresol for novolak (N). The total content of o-o bonded phenolic units, ortho to the hydroxyl groups, is proportional to the p-cresol content of these novolaks. Since the PAC/novolak interaction efficiency is generally increased by the presence of higher levels of the novolak o-o bonding,[3] it is expected that novolak (N) based resist formulations would exhibit greater inhibition than novolak (F) formulations. Novolak (X) is an experimental novolak designed to provide higher PAC/novolak interaction efficiency than cresol novolaks.

The selected PACs were: 1) a monofunctional PAC (M), 2) a tri-functional, partially esterified PAC (T), and 3) a 7-functional, partially esterified PAC (P). These PACs were prepared by forming esters of 2,1-diazonaphthoquinone (DNQ),5-sulfone with, 1) phenol, [PAC (M)], 2) a 50% DNQ ester with 2,3,4-trihydroxybenzophenone (THBP), [PAC (T)] and 3) a 65% DNQ ester with 2,6-bis[1,2,3-trihydroxy,6-methylenephenyl],4-methylphenol (7PY), [PAC (P)]. With the exception of the monofunctional PAC (M), which is a 99% pure compound, PACs (T) and (P) are mixtures of isomers as judged by liquid chromatography. PAC (T) is a mixture of about 50% of the 3D, fully esterified, 20% di-ester, and 10% mono-ester THBP isomers with about 20% unesterified THBP. PAC (P) consists of 12% of the 7D fully esterified, 70% 6D ester and 18% of lower esterification isomers of 7PY.

Table I provides the experimental resist matrix prepared with these novolaks and PACs. The dissolution rates of each of the novolaks used in this study was measured and is also reported in Table I.

Table I. Experimental resist formulation identification

		PAC WEIGHT% IN RESIST DRY FILM									
PAC	DR*	15%T	22.5%T	30%T	12%P	16%P	20%P	8%M	10%M	14%M	18%M
N	168	15NT	22NT	30NT	12NP	16NP	20NP	8NM	10NM	14NM	18NM
F	695	15FT	22FT	30FT	12FP	16FP	20FP	8FM	10FM	14FM	18FM
X	522				12XP	16XP	20XP				

*DR= Novolak dissolution rates in Ångstroms/second

2.3 DRM and Raw Data Analysis

The dissolution rate data was collected in immersion development using a Perkin Elmer DRM unit. The developer used was a 0.262 N aqueous solution of tetramethylammoniumhydroxide (TMAH). Silicon wafers were spin coated using an SVG wafer track and soft baked at 90 °C for 60 seconds. A GCA 0.30 NA g-line stepper was used to expose the resist coatings. Sixteen separate open frame exposures (zones) were made per wafer, ranging from unexposed to 1200 mJ/cm^2. A post exposure bake at 115 °C for 60 seconds was applied for all wafers. Development times as long as 5000 seconds were necessary to obtain sufficient film loss in low exposure zones. The raw data was reduced to 16 sinusoidal waves then transferred to a PC using Perkin-Elmer DRM and SHARE software. Custom software was used for final data analysis with the PC.[4]

3. Results and Discussion

3.1 Data analysis and the significance of model parameters

There are four implicit assumptions in the proposed dissolution model: 1) the dissolution inhibition and enhancement are controlled solely by the inhibitor (M) and the photo-acid (A) concentrations, respectively, 2) PAC conversion is controlled only by a simple photochemical process:

$$M \xrightarrow{\text{light}} A \quad , \qquad (4)$$

so that the sum of the concentrations of the inhibitor and the enhancer is always constant, 3) the dissolution inhibiting and enhancing effects can be applied to the base resin multiplicatively, and 4) the degree of inhibition and enhancement can be given mathematically by effective rate constants and reaction orders as shown in eqn. (1).

Table II lists the measured bulk dissolution rates for both unexposed and totally bleached resists. The effect on dissolution

Table II. Summary of results

				Endpoint measurements						Dissolution curve fits		
	novolak	PAC	Rres	Rmax	Rmin	kinh	kenh	l	n	l	n	Rres
8FM	F	M	695	1452	30.7	1277	18.1	1.6	1.11	3.13	2.43	695
10FM			695	1699	18					1.94	4.75	48.4
14FM			695	2110	13					1.9	5.59	16.5
18FM			695	2584	9.5					1.93	6.03	9.5
8NM	N	M	168	294	7.6	211	2.92	0.89	0.52	0.83	8.77	32.3
10NM			168	317	5.4					0.54	8.86	12.9
14NM			168	354	4.7					0.59	13.06	16.7
18NM			168	362	3.7					0.78	12.69	9
15FT	F	T	695	2398	376	402	17.3	3.27	1.01	7.01	1.74	695
22FT			695	3412	192.7					8.86	2.07	695
30FT			695	4198	54.8					10.9	2.02	695
15NT	N	T	168	563	28.8	1589	52.6	3.06	1.71	7.29	1.56	168
22NT			168	806	9.6					7.52	1.9	168
30NT			168	1321	3.96					5.72	2.34	168
12FP	F	P	695	1242	215.5	66040	15.7	4.86	1.43	4.3	2.6	695
16FP			695	1475	74.5					5.7	4.1	695
20FP			695	1807	18.5					6.5	6	695
12NP	N	P	168	547	1.36	126000	52.6	3.27	1.48	9.35	3.71	168
16NP			168	765	0.54					6.92	4.25	168
20NP			168	983	0.25					6.05	6.62	168
12XP	X	P	522	1136	3.6	1.40E+09	22.3	7.59	1.39	7.01	4.9	522
16XP			522	1426	0.4					7.71	6.63	522
20XP			522	1766	0.1					6.98	7.92	522

rate of the pure inhibitor and the photo-produced acid at various concentrations can be examined by the appropriate plots of the data in Table II; similarly the adequacy of the functional forms assumed in eqn. (1) can be tested by fitting the data to these functions. The appropriate inhibition multiplier taken from eqn. (1) is:

$$(1+k_{inh}\,M^{l})^{-1} \qquad (5)$$

and the enhancement multiplier is:

$$1+k_{enh}(1-M)^{n} = 1+ k_{enh}A^{n} \qquad (6)$$

Assuming for the moment that the concentrations of M and A are given by the fractional PAC loadings, then the plots and fits of Figure 1 can be given. Fig. 1a shows results for the monofunctional PAC (M) in two different novolaks (N) and (F). Fig. 1b shows results for tri-functional PAC (T) in the same novolaks (N) and (F) and Fig. 1c shows results for PAC (P) in the same novolaks as well as novolak (X). The values of the rate constants and orders appropriate to the fits are given in Table II. It is interesting to note that the calculated dissolution enhancement reaction orders cluster around one, while the inhibition orders are generally three or greater.

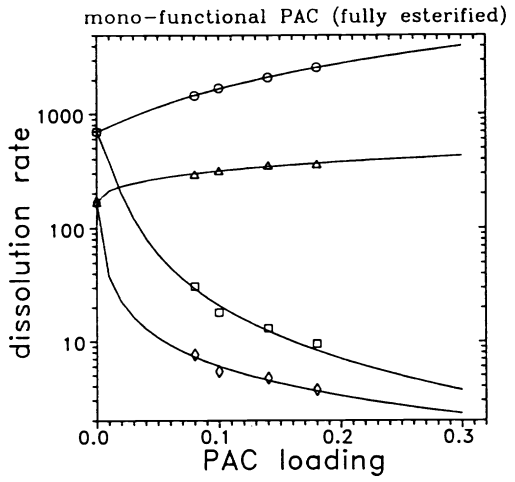

Fig. 1a

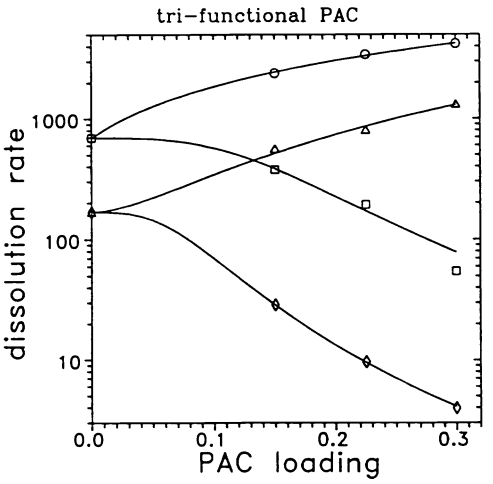

Fig. 1c

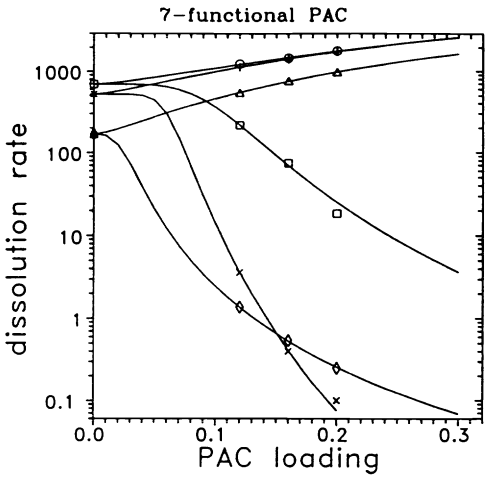

Fig. 1b

Fig. 1 Plots showing the measured dissolution rates as a function of PAC loading (weight %) for formulations containing a) monofunctional PAC, b) tri-functional PAC, and c) 7-functional PAC. In each case the circles and squares plot starting material and fully bleached material, respectively, in novolak F. The triangles and diamonds plot the same measurements in novolak N. The plusses and x's plot the same measurements in novolak X.

Eqn. (1) used in conjunction with the fitted constants allows complete dissolution curves to be calculated for the seven resist systems at any PAC loading. Figures 2-4 show the calculated curves vs. the experimental DRM measurements for each of the 23 formulation/loading combinations. Significant deviation between observed and calculated curves is obvious in almost all of the plots. This generally poor agreement, far beyond the experimental uncertainty, indicates that the dissolution behavior of the calculated resist formulations is more complex than the simple assumptions of the present physically-based model.

In many of the cases examined though, there is reasonably good qualitative agreement between the prediction and experimental. For example, the monofunctional PAC (M) based formulations with novolak (N), Fig. 2b, exhibited the slowest increase in dissolution rate at low PAC conversions experimentally. This result is also predicted by the model although the observed increase is even lower than the prediction. Similarly, PAC (P) formulated with novolak (X) has the greatest increase in dissolution rate for low PAC conversions as shown in Fig. 4c. This too is predicted by the model. An initially steep curve is consistent with a high inhibition order (l) while a flat curve indicates a low rate order.

Secondary inhibition

The apparent deficiencies of the model are traceable to failure in its simplifying assumptions. The idealized photochemistry of process (4) can certainly be faulted because it ignores the possibility of reaction intermediates and side reactions. Products other than the assumed photo-acid may not contribute to dissolution enhancement as expected, and, could even contribute to dissolution inhibition.

The literature provides numerous possibilities for side reactions of the PAC in the resist matrix that would lead to the generation of new dissolution inhibiting products.[5-7] Blum et al.[5] concluded that the resist measured (R_{max}) was more than three times slower than the dissolution rate of an equivalent blend of the novolak and the acid. The blend composition consisted of the same novolak of the resist and a synthetically prepared acid, corresponding to the expected photo-generated acid of the PAC used. They proposed a side reaction between the novolak and the ketene PAC intermediate resulting in a new inhibitor disrupting the dissolution kinetics of the system. Hanabata et al.[6] designed a novolak system that induces PAC/novolak diazo coupling reactions to increase the inhibition of their resist system. Koshiba et al.[7] investigated the possibilities of PAC chemical side reactions that are likely to occur during photoresist processing.

The kinetics of resist dissolution were treated using the same kinetic rules as those of polymer blends by Ushirogouchi et al.[8] They attempted to predict photoresist dissolution curves from measurements of pure inhibitor/novolak and pure photo-acid/novolak formulations. In that work, the specific system chosen for study exhibited purely exponential inhibition and enhancement factors as PAC and photo-product acid loading was varied. Both the inhibition and enhancement effects could therefore be described by single parameters, and, treating the effects multiplicatively without interaction, the following relationship was suggested:

$$\ln[(R(M)] = F\ln(R_p) + (1\text{-}F)(1\text{-}M)\ln(R_f) + (1\text{-}F)M\ln(R_s) \quad . \qquad (7)$$

Here R is the resist bulk dissolution rate, F is the fractional PAC loading, R_p is the resin dissolution rate, M is the conversion normalized PAC concentration, and R_f and R_s are the "apparent" dissolution rates obtained by extrapolating the PAC loading plots to 100% photo-product acid and inhibitor, respectively. Satisfactory agreement between the predicted and measured curves was seen. This approach, however, is not successful for the present system because 1) pure exponential inhibition/enhancement (straight lines in the semi-logarithmic plots of Fig. 1 is not observed, and 2) the subsequent predictions of the dissolution curves using eqn. (7) are also purely exponential while the measured values of Figs. 2-4 show a strong deviation from linearity in the semi-logarithmic plots. The predictions of eqn. (1) are in significantly better agreement with the presently obtained data than the predictions of eqn. (7).

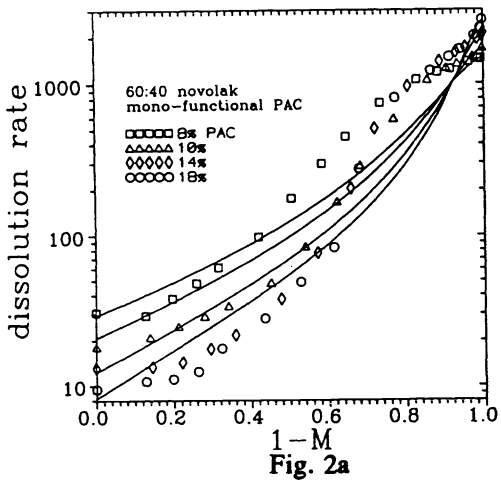

Fig. 2a

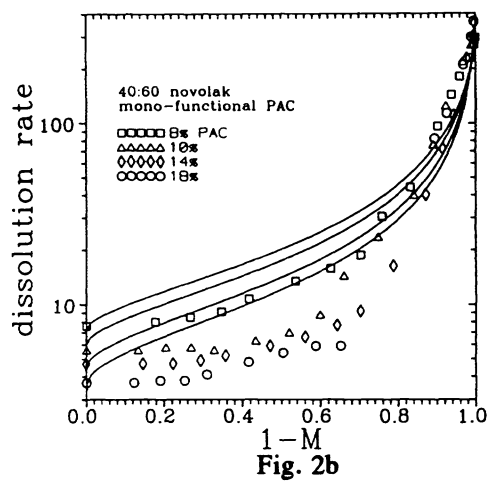

Fig. 2b

Fig. 2 Plot of DRM measured bulk dissolution rates and those predicted by the model and parameters based on the fits in Fig. 1. The monofunctional PAC data is shown in a) novolak F and b) N, respectively. The squares, triangles, diamonds and circles, denote 8%, 10%, 14%, and 18% PAC loadings, respectively.

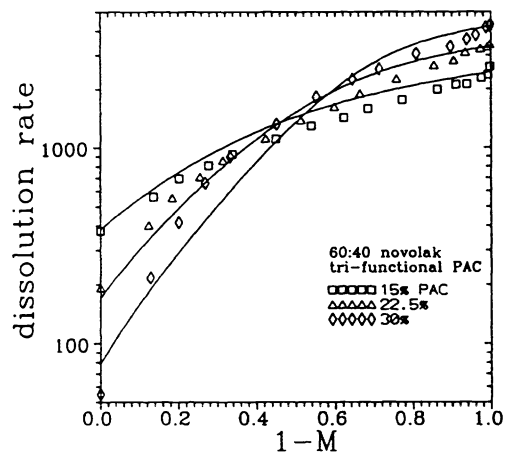

Fig. 3a

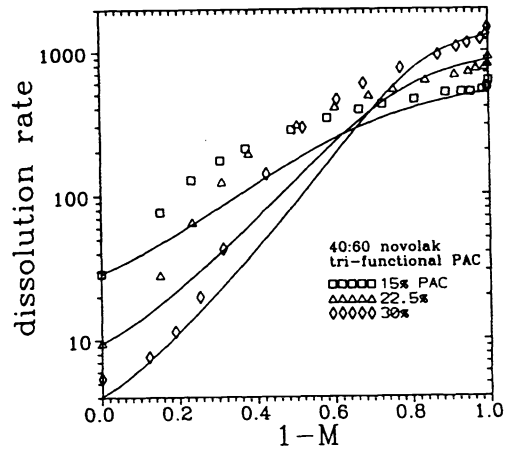

Fig. 3b

Fig. 3 As in Fig. 2 except the tri-functional PAC was used. The squares, triangles, and diamonds, denote 15%, 22.5%, and 30% PAC loadings.

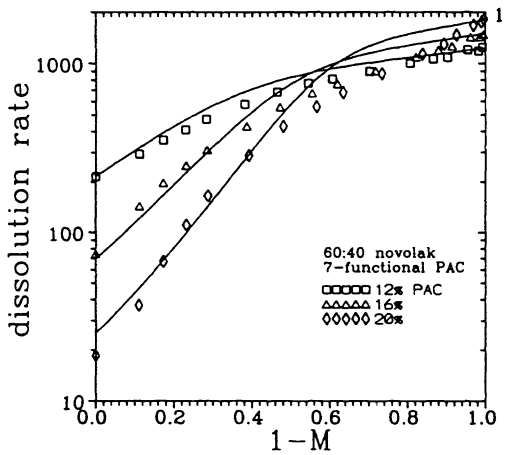

Fig. 4a

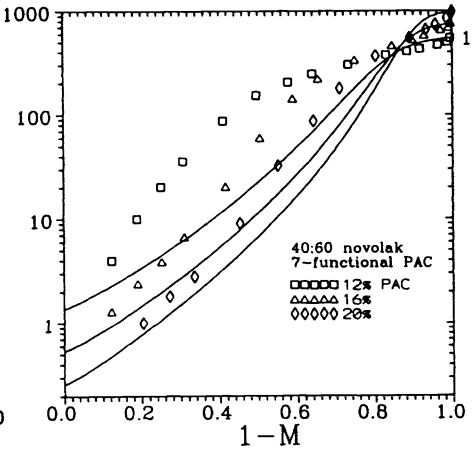

Fig. 4b

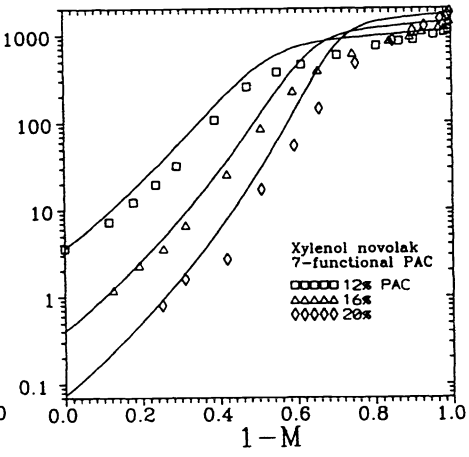

Fig. 4c

Fig. 4 As in Fig. 2 except the 7-functional PAC was used and the loadings are 12%, 16%, and 20%. c) used novolak X.

Polyphotolysis

The photochemistry of process (4) treats each photo-active moiety as a separate decoupled entity. The model does not distinguish between the inhibition/enhancement characteristics of different PAC isomers of polyfunctional PACs.[9] PACs containing isomeric mixtures of the same backbone structure are not identical in their dissolution properties to single isomer PACs of the same backbones and the same DNQ contents.[10] On this basis, the simplification of the photochemistry to process (4) can be easily challenged on physical grounds. An obvious generalization of eqn. (1) is:

$$R(M) = R_{res} * \Sigma f_i \{[1 + k_{enh}(1-M)^n / (1 + k_{inh} M^l)\} \qquad (8)$$

where the sum is over all PAC isomers of fractional concentration f_i, and includes constants for the dissolution inhibition and enhancement characteristics of each. Unfortunately, it is impractical to measure all of the individual rate constants and reaction orders, and furthermore it is inadvisable to use such a large number of parameters to describe resist dissolution, physically-based or not. In fact, the data suggest that these concerns may not be at the heart of the discrepancy, because a substantial disagreement exists between observed and calculated dissolution curves even for single isomer monofunctional PAC systems, as shown in Fig. 2, and seen by others.[10]

The failure of the model to exactly account for the dissolution behavior of the monofunctional PAC systems implies that either reaction intermediates or side-products are important, or, that the assumption that inhibition and enhancement can be treated independently and multiplicatively, is in error. Of these two possibilities, the second is perhaps more likely. Taking the specific case of the 18NM formulation, after 50% photolysis its dissolution rate increases only to about 5 Å/sec from the unexposed value of 4 Å/sec. This material nominally contains 9% PAC and 9% photo-acid. For comparison, the 8NM formulation which dissolves at 7.6 Å/sec with 8% PAC loading and 294 Å/sec upon complete conversion, can be used. It is clear that the half-bleached 18NM system is not experiencing any dissolution enhancement, the remaining PAC functioning as a barrier to dissolution, apparently independent of any influence by the photo-products.

Diffusion mechanism

Another approach to understanding dissolution kinetics involves diffusion. The dissolution rate determining step according to this model[11] is the diffusion rate of the base into the resist film. Initially the base molecules penetrate the resist solid surface and deprotonate the phenolic novolak. This allows water molecules to enter the resist surface more easily and gradually a gel intermediate phase is formed between the resist solid film and the developer solution. This phase is called the penetration zone. As the protonated novolak molecules become soluble in water they leave the penetration zone and enter the developer solution. The chemistry, depth, concentration profile and other properties of this zone are key elements in understanding the total dissolution model. It is likely that within the penetration zone that other inhibition mechanisms take place. Examples of such mechanisms are TMAH ion complex formation[12,13] or surface deposition of insoluble material[14] and the build up of less soluble material on the surface. A completely successful kinetic dissolution model for positive novolak-based resists will probably need to include diffusion aspects.

A diffusion-based model of dissolution may be able to account for the behavior exhibited by the monofunctional PAC systems discussed in the previous section. If the increase in the penetration zone thickness (swelling) is equal to or greater than the loss of total resist thickness at low exposures, such behavior will result. This may be a good explanation, however, it has not been confirmed by experimental data.

3.2 Empirical Fitting with the 5-Parameter Rate Equation

As resist formulators strive to improve lithographic performance, the dissolution curves associated with the new materials can sometimes take on unusual shapes. The accuracy of computer simulations involving these systems may be limited by the inability of the dissolution rate equation to faithfully describe the data, and, as mentioned

earlier, the 3 and 4 adjustable-parameter models in common use are inadequate for many systems. It is of interest to determine whether the 5-parameter model under discussion here offers substantial improvement in this area.

A bulk dissolution curve for HiPR-3512 photoresist in OPD-262 developer (0.262 N TMAH, both are products of OCG Microlectronic Materials, Inc.) along with fits to a standard 4-parameter[15] and the present 5-parameter model are shown in Fig. 5. In each case the fits were done to minimize the sum of the squared deviations from the semi-log plot shown. It is not surprising that the extra adjustable parameter in the 5-parameter model allows a better fit, but in this case the difference is dramatic: the 4-parameter fit is poor, while the 5-parameter fit is excellent.

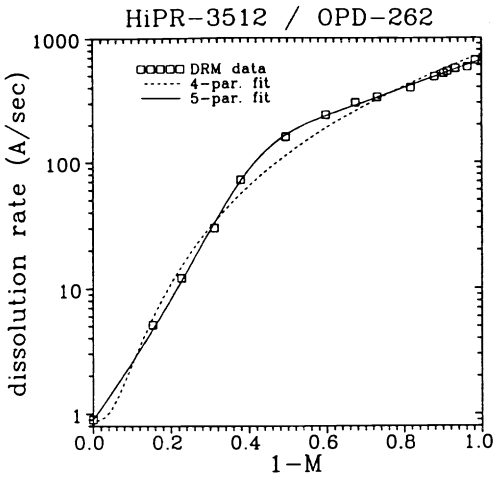

Fig. 5 Plot of DRM-measured bulk dissolution rate data for HiPR-3512 resist in OPD-262 developer along with the best fits given by Mack's 4-parameter and 5-parameter rate equations.

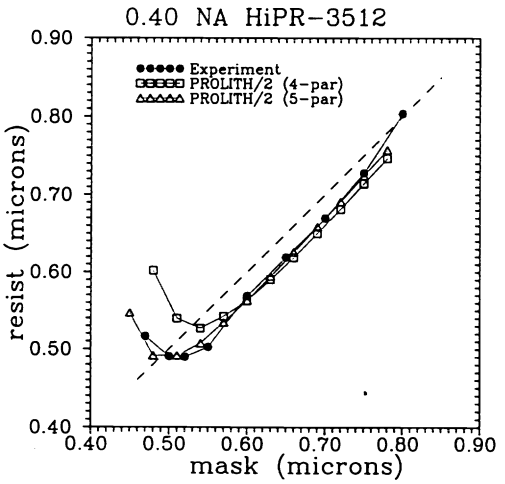

Fig. 6 Lithographic measurements of HiPR-3512 mask linearity along with PROLITH/2 predictions using the bulk dissolution curves of Fig. 5.

Simulations performed with the two fitting curves of Fig. 5 predict significantly different lithographic performance. Using a custom version[16] of PROLITH/2 to calculate line/space pair mask linearity compared with actual measurements on a 0.40 NA i-line stepper leads to Fig. 6. The experimental exposure dose was 131.2 mJ/cm² while the simulations used 145 and 155 mJ/cm² for the 5-parameter and 4-parameter simulations, respectively. The main points of Fig. 6 are that the 4 and 5-parameter models predictions are noticeably different, and, that the 5-parameter fit, which accurately describes the raw dissolution curve, also accurately simulates the observed lithographic performance. This example demonstrates the importance of accurately importing the raw dissolution curve into the simulator, and the ability of the Mack 5-parameter model to do so.

Fig. 7 illustrates the ability of the rate equation to empirically fit typical dissolution curves taken from the previous section. The parameters used to generate best fits of the curves are listed in Table II. The R_{res} values used to fit the monoester based resists had to be adjusted to lower values than the measured rates for the novolaks. In addition, the degree of reduction of this parameter from the measured values appear to be related to the PAC loadings. Comparing the reaction orders l and n for both methods (best curve fit and end point based calculations), one can detect quantitative differences in inhibition and enhancement for each resist. Large differences reflect strong deviations from the idealized model. Such trends carry hidden information related to the complexity of the different mechanisms that determine the resist dissolution behavior.

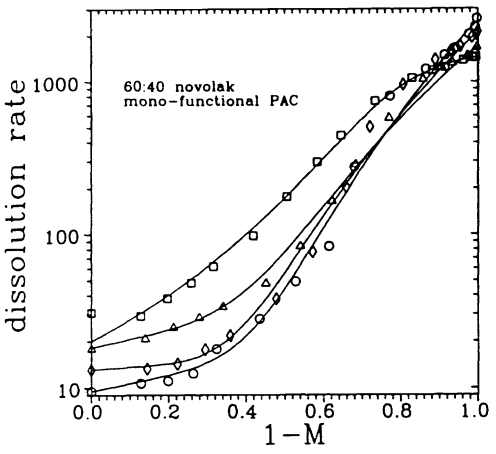

Fig. 7a

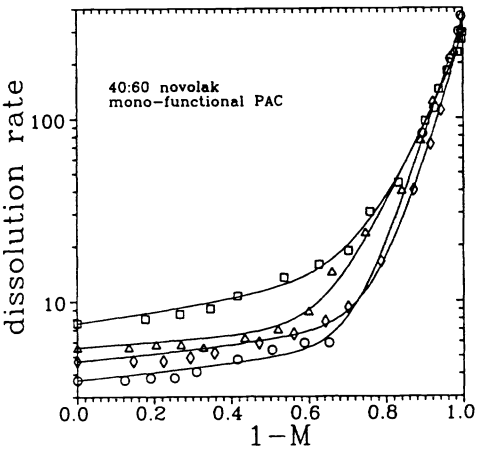

Fig. 7b

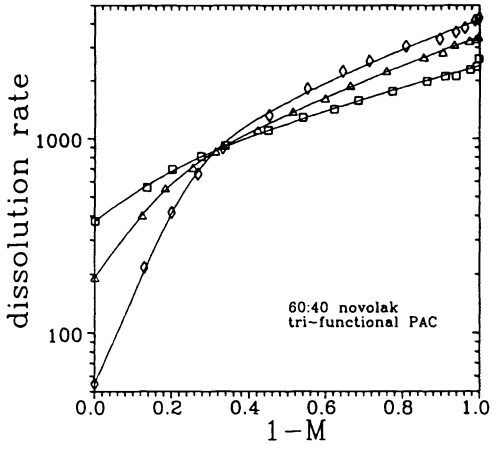

Fig. 7c

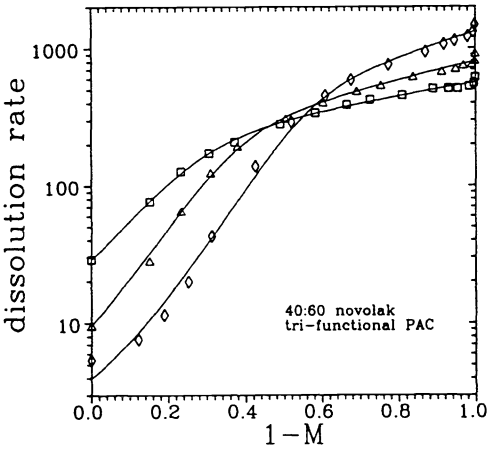

Fig. 7d

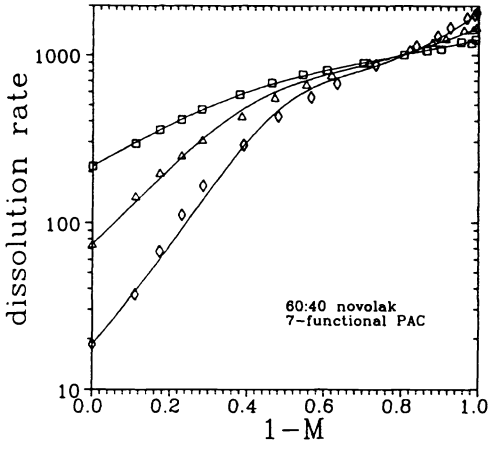

Fig. 7e

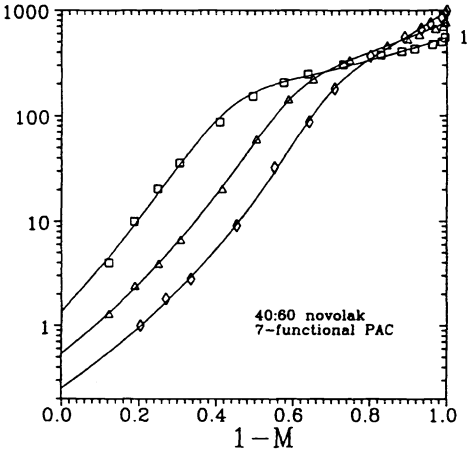

Fig. 7f

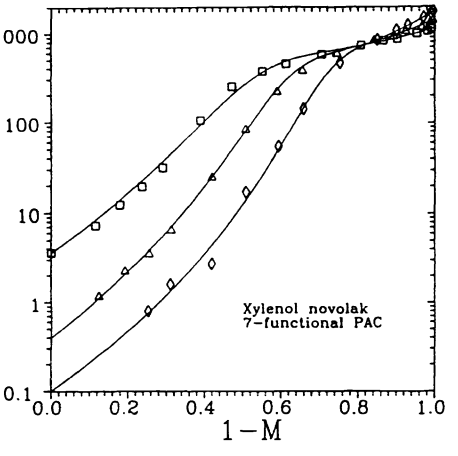

Fig. 7g

Fig. 7 Plots as in Figs. 2-4 but showing best fits to the raw DRM data using equation (1).

The dissolution rate of the resin in some resist formulations may not be the exact parameter to be used in eqn. (1). That is, if the formulation contains non-photoactive additives that accelerate or inhibit the dissolution of the resin then a better value to use is the measured one for the mixture of the resin and that additive at the same concentration as in the resist formulation. This value is the resist dissolution base line, from which inhibition or enhancement, as a function of PAC loading and photolysis, operates. Compounds containing organic acids and/or

anhydride functionalities as well as hydroxyphenyl type compounds are usually considered dissolution enhancers, depending on the dissolution rate of the novolak and the developer normality. Compounds lacking the acidic functionality but containing highly polar groups may not act as strong dissolution enhancers, but they are also not considered inhibitors because of their hydrophilicity. Compounds that are neither acidic nor water soluble are likely to be inhibitors. Additives are frequently used in commercial resist formulations. Examples of such additives are organic dyes, adhesion promoters, surfactants or even unesterified hydroxyphenyl type compounds present in the PAC mixture itself.

4. Conclusions

Mack's new physically-based 5-parameter model for positive photoresist bulk dissolution shows interesting qualitative agreement with several test systems examined in this work, but fails to quantitatively describe their dissolution characteristics. The most likely explanations for the quantitative difficulties are: 1) the assumptions that inhibition by the PAC and enhancement by the photo-acid can be treated independently and multiplicatively apparently fail, 2) side reactions and intermediates are neglected, and 3) complex PAC isomeric distributions and associated complex inhibition/enhancement effects are also neglected. More work is necessary before it can be decided whether the qualitative successes of this dissolution model will be valuable in guiding resist formulation.

The model does exhibit excellent flexibility in fitting actual bulk dissolution rate curves. This reason alone is sufficient to recommend its inclusion in commonly-used simulation programs such as PROLITH/2 and SAMPLE. The present work shows that significant errors can result by using simpler dissolution rate equation which are unable to accurately describe observed bulk dissolution data.

5- Acknowledgement

The authors would like to acknowledge their colleagues, especially A. Jeffries III and J. Ferri for their valuable assistance, K. Honda for pointing out Ref. 8, and G. Dao for providing a useful translation.

6. References

1. Ohfuji, T., Yamanaka, K., Sakamoto, M.,"Characterization and modeling of high resolution positive photoresists", Proc. SPIE 920, 190 (1988).
2. Mack, C., "New Kinetic Model for Resist Dissolution", submitted for publication.
3. Honda, K., Beauchemin Jr., B., Hurditch, R., Blakeney, A., Kawabe, Y., Kokubo, T., "Studies of the molecular mechanisms of dissolution inhibition of positive photoresist based on novolak-DNQ", Proc. SPIE 1262, 493 (1990).
4. Hansen, S.G, Dao, G., Gaw, H., Qian, Q.-D., Spragg, P., Hurditch, R.J., "Study of the relationship between exposure margin and photolithographic process latitude and mask linearity", Proc. SPIE 1463, 230 (1991).
5. Blum, L., Perkins, M. E., McCullough, A. W.,"A study of dissolution kinetics of a positive photoresist using organic acids to simulate exposed photoactive compounds", Proc. SPIE 771, 148 (1987).
6. Hanabata, M., Furuta, A., Uemura, Y., "Novolak design for high resolution positive photoresists", Proc. SPIE 771, 85 (1987).
7. Koshiba, M., Murata, M., Matsui, M., Harita, Y., "Thermally induced and base catalyzed reactions of naphthoquinone diazides", Proc. SPIE 920, 364 (1988).
8. Ushirogouchi, T., Onishi, Y., Kumagae, A., "A new resist profile simulation on the basis of analysis on dissolution properties of resist components", J. Photopolym. Sci. Technol. 2, 76 (1989).
9. Trefonas III, P., and Daniels, B. K., "New principle for image enhancement in single layer positive photoresist", Proc. SPIE, 771, 194 (1987).
10. Uenishi, S., Sakaguchi, S., Kawabe, Y., Kokubo, T., Toukhy, M., Jeffries III, A., Slater, S., Hurditch, R., "Selectively DNQ-esterified PAC for high-performance positive photoresists", Proc. SPIE, 1672, 1992.
11. Yeh, T., Shih, H., Reiser, A., Toukhy, M., Beauchemin Jr., B.,"A quantitative description of dissolution and discrimination inhibition in novolak and other phenolic resins", submitted for publication.

12. Itoh, K., Yamanaka, K., Nozue, H., Kasama, K., "Dissolution Kinetics of High Resolution Novolak Resists", Proc. SPIE, 1466, 485 (1991).
13. Honda, K., Beauchemin Jr., B., Hurditch, R., Blakeney, A., Kokubo, T., "Studies of dissolution inhibition mechanism of DNQ-novolak resists: part III, secondary inhibition with quaternary ammonium salts in development process", Proc. SPIE, 1672, 1992.
14. Furuta, M., Asaumi, S., Yokota, A., "Mechanism of dissolution inhibition of novolak-diazoketone resist", Proc. SPIE, 1466, 477 (1991).
15. The original Mack 4-parameter model
$$R = R_{max}\{(a+1)(1-m)^n/a(1-m)^n + R_{min}$$
was used and is described in: Mack, C.A., "Development of positive photoresist", J. Electrochem. Soc., 134, 148 (1987).
16. This version allows the import of arbitrarily shaped bulk dissolution curves.